Resistivity structure of the central part of the Yamasaki fault studied by the multiple electrodes resistivity method

Kiyoshi Fuji-ta and Osamu Ikuta*

Department of Earth and Planetary Sciences, Kobe University, Rokkodai 1-1, Nada-ku, Kobe, Hyogo 657-8501, Japan

(Received November 8, 1999; Revised June 21, 2000; Accepted June 26, 2000)

The Yamasaki fault system is a well known major, active fault in South-Western Japan. Large historical earthquakes have occurred along it. Several resistivity models of the Yamasaki fault have been proposed as the result of intensive electromagnetic investigations during the 1970's and 1980's. In 1996, a trench study was made of the cross-section of the Yasutomi fault which is the kernel of the Yamasaki fault system. The cross-section showed the occurrence of past major paleo-earthquakes. To clarify the deeper structure of the fault, multiple electrode resistivity soundings were conducted across the fault in 1997. Although the target sounding depth of the previous EM survey is different, the resistivity measurements show the boundary structure of the central part of the fault beneath the trench survey area. They also show the extent of a shallow conductive zone across the fault.

1. Introduction

The Yamasaki Fault system is noted for its activity and has been recognized as one of the major active inland faults in South-Western Japan. It extends over 80 km and its strike direction is almost NW-SE. Along the Yamasaki fault earthquakes of magnitudes 5 and above have been observed (Research Group for Yamasaki Fault, 1988a, b). In particular, in 1984, an earthquake of magnitude 5.6 occurred in the central part of the fault. Because this fault is active, it has been used as a test area for many geophysical projects designed to examine the possibility of earthquake prediction (Research Group for Yamasaki Fault, 1988a, b). Prior to these projects, observations were made between 1975 and 1978 using measurements of the total magnetic force, very low frequency (VLF), extremely low frequency (ELF) magneto-telluric methods, the direct current method, and other Electro-Magnetic (EM) methods (e.g. Electromagnetic Research Group of the Active Fault, 1982; Handa and Sumitomo, 1985; Sumitomo and Noritomi, 1986). These studies showed the resistivity structure to a depth of about 10 km and found that a low resistivity zone runs along the fault which is presumed to be the fault-fractured zone with a high water content (Electromagnetic Research Group of the Active Fault, 1982). However, the accurate shape of a low resistivity zone was not imaged. Furthermore, the influence of the surface water and/or ground water of a low resistivity zone was not clear.

The Yamasaki fault is a left-lateral strike slip fault (Watanabe, 1991a, b). The Yasutomi fault is located in the central part of the Yamasaki fault system. The displacements and dislocations produced by past earthquake activities along the Yasutomi fault, are distinct. To inspect the past records of earthquakes, a trench survey was conducted across the center of the Yasutomi fault in 1996. It revealed the occurrence of at least five major paleo-earthquakes during the past 24,000 years to a depth of 10 m. The averaged lateral slip rate was estimated to be less than 1 mm/year (Hyogo Prefectural Government, 1996).

We focused on the Yasutomi fault which is the kernel of the Yamasaki fault system (Fig. 1(a)), and applied a multiple electrode array and analyzed the data. Our motivation for this study is to determine the location and precise shape of the fault zone of the Yasutomi fault. It is essential to study its shallow resistivity structure. In the present paper, preliminary results of the study of the resistivity structure are described, showing the existence of two remarkable conductive zones which cross the Yasutomi fault.

2. Multi-Electrode Resistivity Sounding

In this study, electrical resistivity data were collected using a McOHM-21 (OYO-Corp.) system and geo-electric scanner that went with it. In the case of pole-pole array configuration used here, two electrodes are fixed while one potential and one current electrode are selected in a variety of electrode configurations.

The electrical resistivity survey was carried out in December 1997. The resistivity cross-sections are almost perpendicular to the strike of the fault (Fig. 1(b)). Electrodes were arranged along the profile in advance. To avoid the electrical distortion from the near-surface, the survey area was selected to be within relatively homogeneous geology. Typically, 32 electrodes were laid out along the profile with a spacing of 3 or 4 m so that the total length of the profile was either 93 or 124 m. The observation profiles are illustrated in Fig. 1(b). Two remote electrodes were placed a long distance from the profile. One remote electrode played the role of the infinite distance current electrode and, on the opposite side of the array, the other one played the role of the potential electrode.

*Now at Sumitomo Bank Ltd.

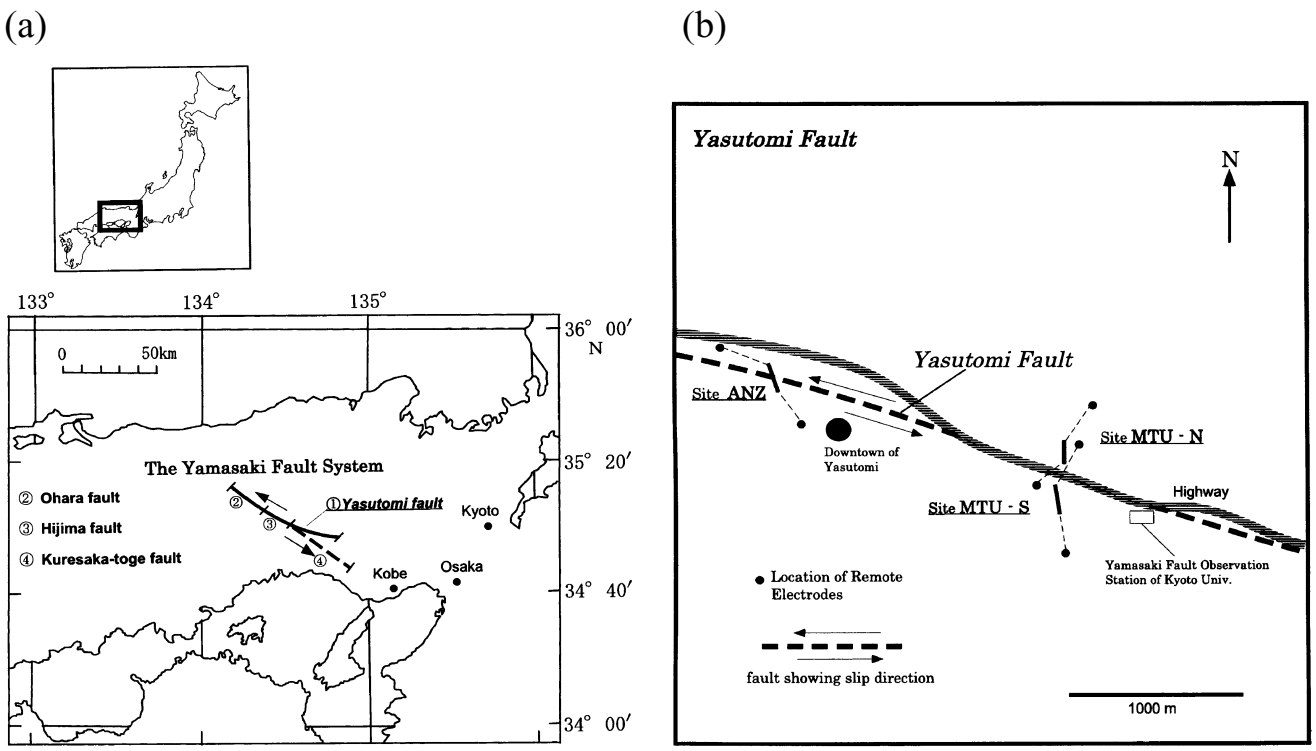

Fig. 1. (a) Location map showing the Yamasaki fault system. Yasutomi fault is situated in the middle of the Yamasaki fault system. (b) Configurations of Multi-Electrodes Resistivity profiles. An Anzi (ANZ) profile is designed to cross the Yasutomi fault. Mitsumori-North (MTU-N) and Mitsumori-South (MTU-S) profiles are separated to avoid the effect of the highway and its base.

To overcome high contact resistance, we poured a saline solution around the electrodes or two or three extra electrodes were added. An electric current was applied to the ground as a symmetric square wave at a period of 1.6 sec and the corresponding potential records were stacked for ten periods. The maximum DC current was 200 mA. The ratio of the output voltage to the input current *V/I*, was calculated. The first measurement was conducted with its centre between electrode Nos. 1 and 2, then Nos. 1 and 3, Nos. 1 and 4, and so on (Fig. 2). The measurements totaled up to 360.

The measurement device was equipped with a notch filter of 60 Hz to avoid noise from commercial power lines. Before the measurement, self-potential values and background noise were also monitored to prevent bias in the data. With the above preparation and precautions, high-quality data was obtained.

3. Data and Modelling

In general, electrical potential in a uniform earth decreases along the profile in an inverse proportion to the distance from the current electrode. Observed resistivity values were plotted on a linear graph as a function of distances along the electrodes. To avoid measurement errors, these attenuation curves were checked by visual inspection at the field sites. When the data showed a large error bar and scatter for some points, duplicate or triplicate measurements were conducted. As Zohdy (1989) pointed out, noise in the data can produce anomalous layers. Data that indicated more than 5 percent errors were excluded.

We have compiled data as a pseudo-section and contoured (e.g. Apparao, 1997). Figure 2 shows an example of a pseudo-section along the Anji (ANZ) profile. After inspecting each of the pseudo-sections, resistivity data were used for two-dimensional analysis.

Two-dimensional inversion was used for interpreting the resistivity sounding curves (Shima *et al.*, 1995). The analysis program uses the Finite Element Method (FEM) and can include a topographic correction. The modelling process contains the following steps.

At the first step in the initial model, we assumed that the subsurface layer was homogeneous with a uniform resistivity. Topographic compensation was applied by multiplying the data by the corrected coefficients of the topography which was modelled to include the detailed undulation of the surface. With this procedure, any interactive influence between the topography and the subsurface structure can be effectively compensated (Shima, 1990 and 1992). Since the geological strike is predominantly two-dimensional in these regions, the data are matched by the iterative use of the two-dimensional FEM.

Secondly, in the case of no data, an averaged value was interpolated. The error floor of the data was 10% and they were equally weighted in the inversion. The horizontal resolution in the analysis is defined by the inter-electrode spacing, and the vertical resolution by a half of it (e.g. Reynolds, 1995). In the trapezium-shaped resistivity model, the horizontal length of surface profile was 93 or 124 m and the maximum depth was 45 or 60 m, respectively.

To test the model resolution, the convergence of the precision parameter was checked. The iterative procedure was performed to minimize the averaged residuals between the observed (*V/I*) and calculated values. As a result, the resid-

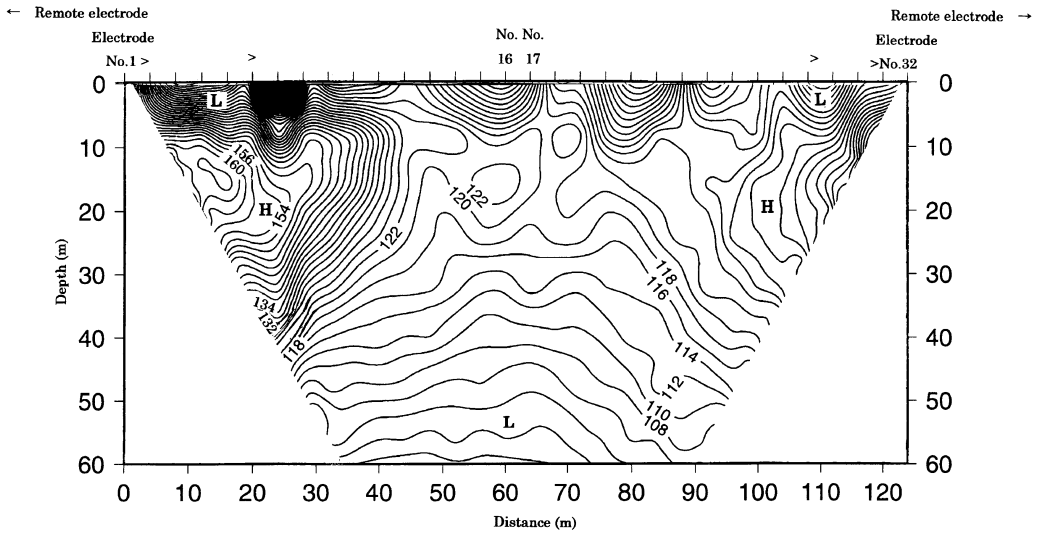

Fig. 2. An example of the pseudo-section of resistivity obtained along the Anzi (ANZ) profile and its electrodes arrangements. Resistivity contours are at 2 Ωm intervals.

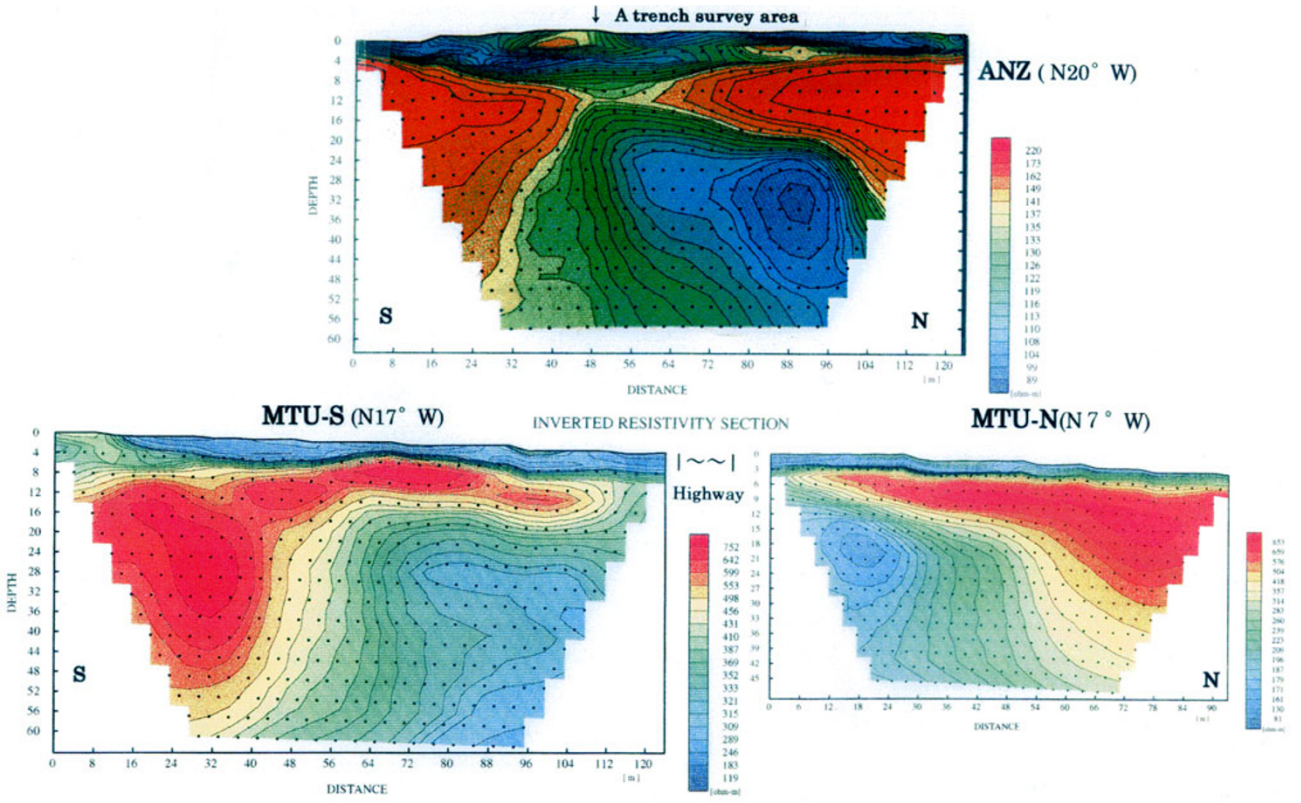

Fig. 3. (a) Resistivity cross-section of site ANZ (Top center). (b) Resistivity cross-section of site MTU-N (Right bottom). (c) Resistivity cross-section of site MTU-S (Left bottom). All figures are illustrated using a natural scale (V : E = 1 : 1). Dots show data points.

uals become small for each computation. The sum of the squares of the residuals between the measured values and the theoretical values was minimized. The final averaged residuals were 0.0029 for profile MTU-S, 0.0022 for profile MTU-N, and 0.0016 for ANZ profile which were less than a few percent of those for the initial model. As the result, the layered structure for all profiles were well resolved.

4. Electrical Resistivity Structure of the Yamasaki Fault

The variation in the magnitude of apparent resistivity highlights several anomalous areas along the profiles (Figs. 3(a), (b), (c)).

The modelled resistivity cross-section of the Anji (ANZ) site is shown in Fig. 3(a). The near-surface stratification is relatively horizontal and continuous except for the middle of the profile. Along all three profiles, the geology consists

of near-surface terrace deposits overlying a gravel basement. Modelling shows the near-surface layer has low resistivity, while the basement rocks have resistivity as high as 200 Ωm. Note that the model consists of an inclined fault zone with a resistivity of less than 100 Ωm (blue colored) at the center of the profile extending to about 15 m beneath the surface. The profile crosses the 10 m deep trench surveyed by another group (Hyogo Prefectural Government, 1996). The two investigations cannot be directly compared because the resolution and sounding depths are different. Nevertheless, it is clear that a conductive zone, which corresponds to the fault zone, is just below the excavation by the trench. The present survey successfully detected the fault zone at the central part of the Yasutomi fault to a depth of 60 m. The conductive fault zone marked by a resistivity of less than 100 Ωm intrudes into the basement with a north-ward dip. The cross-section along the ANZ profile shows the well resolved fault zone but, because of the modelling edge effect, it is difficult to resolve the deeper part of the fault.

The Mitsumori profile consists of two separated electrodes arrays MTU-N and MTU-S shown in Figs. 3(b) and (c). The profile was measured in two parts to avoid the effects of artificial constructions in particular the highway and its base. Although the profile is interrupted by the main highway (less than 70 m in width) and the strike directions of the two profiles are slightly different, the deep structure of Yasutomi fault, which runs below the highway, was successfully detected. Continuous and related structures were found in spite of the lack of data between the profiles. In addition to the terrace deposit of low resistivity with a thickness of 5 m, both profiles show the basement with a resistivity of more than 500 Ωm. In addition, comparing the two cross-sections, it can be seen that widespread conductive zones with resistivities of less than 150 Ωm surround the fault. Since these conductive zones have almost the same resistivity values, we suggest that they are continuous layers of conductive material surrounding the fault. These conductive zones (blue-green colored) which are clearly associated with the fault structure, were also observed by the Electromagnetic Research Group of the Active Fault (1982).

The three resistivity profiles all show low resistivity zones with different shapes and thicknesses beneath about 15 m. Such conductive zones are often found to be associated with strike slip faults (e.g. Unsworth *et al.*, 1999).

In general, the fault gouge is very thin (e.g. Lin *et al.*, 1998), the width being less than about 1 meter. Since the low resistivity zones found in this study are thick and complicated, we cannot identify the low resistivity zone with the gouge itself. Another cause of low resistivity zones must be sought.

The Electromagnetic Research Group of the Active Fault (1982) observed a deeper structure along the Yamasaki fault system and concluded that the conductive layers along the fault are the fracture zone which has a high content of water. They suggest that rocks have been fractured along the fault during the past major earthquakes or the current movement of the fault. In this case, rocks along the fault became porous and water supplied from ground fluids and/or rainwater filled the loosed structure, resulting in the conductive fracture zone along the fault.

Along the fault zone, the presence of cataclasite may be another cause of the conductive zone. Cataclasite can occur in a wide-spanning belt across the fault. Scholz *et al.* (1993) suggested that cataclasite zone may be the result of pulverization due to the repeated passage of the crack-tip stress field from many earthquakes. Since the rocks of the Yasutomi fault have been deformed for a long period, large compression or friction of the fault has induced the thermal effects and alteration. If the cataclasite has a high content of clays and the thermal effects have continued for a long time, this zone will be highly conductive. Therefore, cataclasite is an another important candidate for the fault zone as it increases the conductivity. However, to identify the cataclasite, the grain size and proportion of the matrix must be inspected and classified (Sibson, 1977). In any case, it is clear that we need mere geological information of the Yasutomi fault and further microscopic inspections of the fault rocks.

5. Conclusions

In this study, two unusual structures were found across the Yasutomi fault of the Yamasaki fault system. An inclined and conductive fault zone of less than 100 Ωm in resistivity was found at the Anji (ANZ) profile. It is situated at depths of between 15 and 60 m. This conductive zone is located just below the excavation trench. Although the Mitsumori profiles (MTU-N and MTU-S) are separated by a large highway, they show continuous and related structures. A continuous conductive zone can be seen between the two profiles. It is shallow and approximately 200 m in width and is believed to be the crushed or altered zone of the Yasutomi fault.

The present results are consistent with the electromagnetic observations of the Electromagnetic Research Group of the Active Fault (1982), but the target-sounding depth in this survey is shallower to allow a more precise analysis of the associated structure. It has been shown that the models of resistivity derived from multiple electrode resistivity surveys are good indicators of the extent of the fractured rocks and/or alteration products along the fault. This method can identify the associated complex structure of the fault. The present results are preliminary and more profiles are necessary at other sites across the fault. To resolve the structure of the fault more accurately, combinations of multiple electrodes resistivity survey with Audio frequency Magneto-Telluric (AMT) and Very Low Frequency Magneto-Telluric (VLF-MT) sounding are desirable.

Acknowledgments. We would like to acknowledge the kind cooperation of the staff of the Yasutomi Town Council in the Hyogo prefecture. K. Watanabe of Kyoto University, A. Lin, and T. Maruyama of Shizuoka University made invaluable comments and suggestions. Y. Makino and K. Ando aided us in preparing the equipment and contributed some of the field work. We appreciate that the OYO-Corporation provided a Mc-OHM21 system, the computer programs and precious computer facilities. We also appreciate that Hugh M. Bibby and an anonymous referee greatly improved the manuscript.

References

Apparao, A., *Developments in Geo-electrical methods*, 293 pp., A. A. Balkema publishers, U.S.A., 1997.

Electromagnetic Research Group of the Active Fault, Low electrical resistivity along an active fault, the Yamasaki fault, *J. Geomag. Geoelectr.*, **34**, 103–127, 1982.

Handa, S. and N. Sumitomo, The geoelectric structure of the Yamasaki and the Hanaori faults, *J. Geomag. Geoelectr.*, **37**, 93–106, 1985.

Hyogo Prefectural Government, *A Brief Report of the Investigation of the Yamasaki Fault, Hyogo Prefecture*, 28 pp., 1996 (in Japanese).

Lin, A., T. Miyata, and T. Wan, Tectonic characteristics of the central Segment of the Tancheng-Lujiang fault zone, Shandong Peninsula, eastern China, *Tectonophys.*, **293**, 85–104, 1998.

Research Group for Yamasaki fault, Review papers of Yamasaki fault (1), edited by Y. Kishimoto, 1988a (in Japanese and English).

Research Group for Yamasaki fault, Review papers of Yamasaki fault (2), edited by Y. Kishimoto, 1988b (in Japanese and English).

Reynolds, J. M., *An Introduction to Applied and Environmental Geophysics*, 796 pp., John Wiley & Sons, 1995.

Scholz, C. H., N. H. Dawers, J.-Z. Yu, and M. H. Ander, Fault growth and fault scaling Laws: Preliminary results, *J. Geophys. Res.*, **98**, 21951–21961, 1993.

Shima, H., Two-dimensional automatic resistivity inversion technique using Alpha centers, *Geophysics*, **55**(6), 682–694, 1990.

Shima, H., A practical 2D Automatic resistivity analysis for pole-pole array Data—Analysis algorithm and applications of "Resistivity Image Profiling", *BUTSURI-TANSA*, **45**(3), 1992 (in Japanese with English abstract).

Shima, H., K. Kajima, and H. Kamiya, *Resistivity Imaging Profiling*, 206 pp., Kokon-shoin publishers, 1995 (in Japanese).

Sibson, R. H., Fault rocks and fault mechanisms, *Journal of Geological Society London*, **133**, 191–213, 1977.

Sumitomo, N. and K. Noritomi, Synchronous precursors in the electrical Earth resistivity and the geomagnetic field in relation to an earthquake near the Yamasaki fault, South-West Japan, *J. Geomag. Geoelectr.*, **38**, 971–989, 1986.

Unsworth, M., G. Egbert, and J. Booker, High-resolution electromagnetic Imaging of the San Andreas fault in Central California, *J. Geophys. Res.*, **104**, 1131–1150, 1999.

Watanabe, K., Strain variations of the Yamasaki fault zone, Southwest Japan, Derived from extensometer observations, Part 1, On the long-term strain variations Derived from strain steps, *Bulletin of the Disaster Prevention Research Institute*, **41**, March, 29–52, 1991a.

Watanabe, K., Strain variations of the Yamasaki fault zone, Southwest Japan, Derived from extensometer observations, Part 2, On the short-term strain variations Derived from strain steps, *Bulletin of the Disaster Prevention Research Institute*, **41**, June, 53–85, 1991b.

Zohdy, A. A. R., A new method for the automatic interpretation of Schlumberger and Wenner sounding curves, *Geophysics*, **54**(2), 245–253, 1989.

K. Fuji-ta (e-mail: fuji-ta@kobe-u.ac.jp) and O. Ikuta